Adsorption (2014) 20:173–188
DOI 10.1007/s10450-013-9561-0

Advanced adsorbents for the separation of the *ortho*- and *para*-hydrogen spin isomers at cryogenic temperatures

Jerome T. Jankowiak · Joseph M. Schwartz · Philip A. Barrett

Received: 17 January 2013 / Accepted: 4 July 2013 / Published online: 18 July 2013

Abstract Improved adsorbent types and compositions have been developed for the challenging separation of the *ortho*- and *para*-hydrogen spin isomers at 77 K. From a systematic study of commercially available adsorbent types, it has been found that zeolites of type X offer the largest capacity and selectivity towards *ortho*-hydrogen and that performance is significantly impacted by the cation type and the number of cations present in the zeolite. For the present separation improved performance was obtained with larger Group I cations, especially K and Cs. Another key property of the adsorbents addressed in the present work is the need to control the adsorbent composition to avoid unwanted catalytic conversion of the *para*- to *ortho*-hydrogen. A common source of unwanted catalytic activity in many adsorbent compositions was identified as the presence of unwanted transition metal impurities, especially iron associated with the natural clays, commonly employed as binding agents in the commercial agglomerated zeolite products. To avoid this, equivalent adsorbent compositions were agglomerated instead using colloidal silica binding agents which successfully minimize back conversion of the *para*- to *ortho*-hydrogen and produced adsorbents with higher capacities and selectivities for the *ortho* component at the test temperature of 77 K. These advanced adsorbents can be applied in more efficient hydrogen liquefaction processes.

Keywords *Ortho*-hydrogen · *Para*-hydrogen · Cryogenic separation · Adsorbent

J. T. Jankowiak · J. M. Schwartz · P. A. Barrett (✉)
Praxair Inc., 175 East Park Drive, Tonawanda, NY 14150, USA
e-mail: philip_barrett@praxair.com

1 Introduction

Normal-hydrogen (n-H_2) is a mixture of 75 % *ortho*-hydrogen (*o*-H_2) and 25 % *para*-hydrogen (*p*-H_2). *o*-H_2 has parallel nuclear spins, while *p*-H_2 has anti-parallel nuclear spins (Silvera 1980). Producing stable liquid hydrogen requires that the *o*-H_2 component in n-H_2 be almost completely converted to the *p*-H_2 form (Schwartz et al. 2011). Even though theoretically *o*-H_2 is thermodynamically stable at liquid hydrogen temperatures, practically collisions with the storage tank walls and/or any trace paramagnetic impurities in the system is sufficient to cause *o*-H_2 to *p*-H_2 conversion. These tank surface and/or impurity mediated conversion reactions are very slow and will take days to approach equilibrium (Anwar 2004). This means that liquid hydrogen sitting in storage tanks will slowly convert from *o*-H_2 to *p*-H_2 (Gursu et al. 1992) and as a consequence of the heat of reaction, vaporization and loss of liquid product will occur.

A catalyst is used in the liquefaction process to ensure that the liquid hydrogen product is near equilibrium (Singleton and Lapin 1965) to avoid conversion of the product in the storage tank and thereby reduce these product vaporization losses. The current liquefaction process incorporates a catalyst in the heat exchanger to convert *o*-H_2 to *p*-H_2 which allows the conversion reaction to take place nearly reversibly, before the product leaves the process (Baker and Shaner 1978). The catalytic conversion occurs over a range of temperatures allowing for conversion at the highest possible temperature, where it is most efficient. In current hydrogen liquefiers *o*-H_2 to *p*-H_2 conversion is responsible for about 20 % of the power consumption.

The equilibrium composition of *o*-H_2 and *p*-H_2 is a strong function of temperature. With reference to Fig. 1

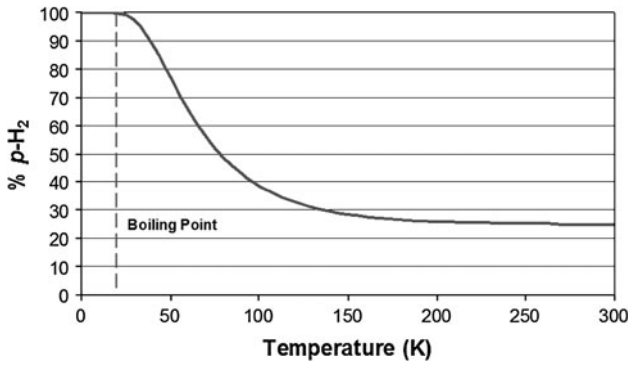

Fig. 1 Equilibrium concentration of p-H_2 as a function of temperature

(Scott et al. 1964), below 150 K, the equilibrium composition changes significantly as the temperature is reduced. The catalyst is not able to produce o-H_2 and p-H_2 mixtures beyond the equilibrium compositional boundary shown in Fig. 1. Once the mixture is allowed to equilibrate in the liquid phase at the boiling point, the composition is effectively 100 % p-H_2. The hydrogen liquefaction process occurs over temperatures that span the entire equilibrium range for o-H_2 to p-H_2 conversion (Schwartz et al. 2011). The heat of the o-H_2 to p-H_2 conversion reaction is also a function of temperature. As can be seen in Fig. 2, the largest heat release occurs at the lowest temperatures (Scott et al. 1964). This means that liquefied n-H_2 would absorb the maximum possible energy release due to o-H_2 to p-H_2 conversion, causing significant boil-off. In fact, the heat of reaction at the boiling point is larger than the latent heat of vaporization. Our calculations have shown that if n-H_2 is liquefied without o-H_2 to p-H_2 conversion, as much as 70 % of the liquid product could be lost by the boil-off mechanism. Because the heat generated, and therefore, the heat that needs to be removed decreases with increasing temperature, one wants to perform the conversion at the highest possible temperature. This reduces the amount of heat that must be removed and allows the heat of reaction

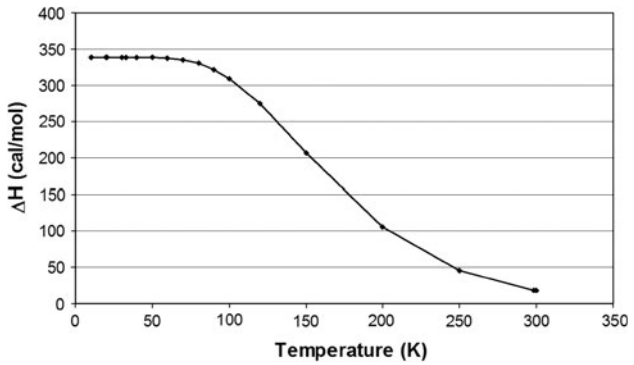

Fig. 2 Heat of reaction for o-H_2 to p-H_2 conversion

to be absorbed at a higher temperature, which increases efficiency.

The use of adsorption technology to supplement the traditional catalytic process for o-H_2 to p-H_2 conversion used in many hydrogen liquefaction processes has been proposed recently (Schwartz et al. 2011). A potential benefit of the adsorption technology is a more efficient liquefaction process, by producing a p-H_2 enriched hydrogen stream at higher temperatures and sending only this p-H_2 rich fraction to the hydrogen liquefier. The o-H_2 enriched waste stream would be warmed to ambient temperature where it can be easily converted to n-H_2 and recycled to the front end of the process. It is envisaged that the adsorption system would comprise at least 2-beds with one bed on feed, carrying out the separation, while the second bed is being regenerated in preparation for the next cycle.

One of the prerequisites for an effective adsorption technology is the identification and/or development of an appropriate adsorbent for the intended separation. o-H_2 and p-H_2 separation has been demonstrated in several publications. For example, Clouter (1972) describes an adsorptive apparatus to separate o-H_2 and p-H_2 and produce o-H_2 in high purity using 1/8 in. activated alumina pellets, at the process temperature of 20 K. The author points out the need to precondition the adsorbents carefully, so as to remove paramagnetic O_2 species, which can promote o-H_2 to p-H_2 inter-conversion. Haubach et al. (1967) reviews the theoretical and experimental data collected by that point in time on hydrogen isomer and isotope separations. One of the conclusions from this review is that classical adsorbents, such as activated aluminas, require operating temperatures near the hydrogen boiling point for the o-H_2 and p-H_2 separation, due to poor separation factors being obtained at temperatures above 50 K.

There are some reports of the use of higher temperatures to effect o-H_2 and p-H_2 separation. For example, Moore and Ward (1958) report that o-H_2 and p-H_2 could be separated chromatographically at 77 K using columns packed with activated alumina adsorbent. Sandler (1954) reported that some degree of separation was achieved at 90 K on rutile titanium oxide and charcoal adsorbents. However, in terms of applying separation technology to improve hydrogen liquefaction systems, chromatographic separation techniques are not feasible at the required scale. o-H_2 and p-H_2 separation under other process conditions and using similar adsorbents have also been disclosed in several papers and articles notably by White and Haubach (1959), White and Lassettre (1960), White et al. (1961), Haubach et al. (1967), (1969), Brillyantov and Fradkov (1957), Van Cauwelaert and Hall (1972), Stevenson and Stevenson (1982).

In terms of the use of zeolites as adsorbents to separate o-H_2 and p-H_2, there are a smaller number of published studies. The separation performance of Na-A zeolite was

studied using computation methods by Anderson et al. (1999) who determined that good separation factors in the range 3–5 can be obtained at temperatures of 50 K and below. Zeolites 4A and 5A were studied both experimentally and computationally for their ability to separate o-H_2 and p-H_2 by Larin and Parbuzin (1992). These authors confirm that the separation occurs and propose some models for the nature of the separation based on rotational freedom and rotational modes for the two hydrogen spin isomers inside the cavities of zeolite A. In a more recent paper by Bystrov et al. (2006), an ultra-pure lithium-exchange zeolite X is studied at 50–112 K using a modified chromatographic separation process. These authors show commercial zeolites are too catalytic, as a result of the presence of detrimental paramagnetic impurities. To address this issue, the authors prepared a higher purity Li-X zeolite powder and used this in a pressed powder form, without addition of any binders or use of any conventional agglomeration techniques, such as extrusion or pan granulation.

The present work seeks to build on the successes reported above, and find ways to make commercial zeolite adsorbents with lower catalytic activity and higher separation factors. In our adsorbent development activities, the goal was to produce agglomerated adsorbent particles which are compatible with classical packed-bed adsorption processes and systems, using traditional shaping or forming equipment that is representative of state of the art commercial adsorbent manufacturing practice. Another aim of the present study was to identify adsorbent compositions based on commercial zeolite precursors having improved capacity and selectivity for o-H_2 at a temperature of 77 K. This temperature was selected since this is easily accessible by cooling with liquid nitrogen and also at this temperature the equilibrium hydrogen composition is close to 50 % o-H_2 and 50 % p-H_2. To meet these objectives, agglomerated adsorbent particles were prepared starting from commercially available zeolite LSX or zeolite A powder obtained from Zeochem LLC. Thereafter, the adsorbents were modified by ion exchange techniques using Group I and II cations. Finally, the performance of the new adsorbent compositions was measured using a custom designed cryogenic breakthrough test system and method. The breakthrough test was preferred since equilibrium, kinetic and catalytic effects will be manifested in this test method.

2 Experiments and methods

2.1 Adsorbent samples and preparation

The materials tested in this study included commercially available materials and adsorbent compositions designed and prepared specifically for this study. The commercial adsorbents were alumina and zeolite Li-exchanged Low Silica X (Li-LSX). In all cases, these materials were obtained from the commercial suppliers, densely packed into the stainless steel test beds, and subjected to activation pre-treatments, depending on adsorbent type. For alumina, samples were activated for 4 h, under dry nitrogen at a temperature of 250 °C and for the Li-LSX, the activation conditions were 8 h under dry nitrogen at 350 °C. A commercial hydrated iron oxide o-H_2 to p-H_2 hydrogen conversion catalyst was obtained from Molecular Products Inc. for use as a reference and also to equilibrate the n-H_2 feed gas to the 50 % o-H_2 and 50 % p-H_2 equilibrium composition expected at 77 K.

A number of adsorbent compositions were prepared in agglomerated form from commercially available zeolite powders. The intent was to have more control over the adsorbent compositions and, in particular, the levels of paramagnetic impurities, which are suspected to increase the catalytic activity and reduce the effective separation (Bystrov et al. 2006). The core steps involved are depicted in Fig. 3. In general terms, the adsorbent component was blended together with a binder and any required processing aids. For the binding agent, Ludox LS30 colloidal silica was used, since this has been shown to produce shaped adsorbent particles with adequate crush strength and low mass transfer resistance by Zheng et al. (2008). Another motivation for the selection of colloidal silica, as the binding agent was to reduce the amount of paramagnetic impurities, such as iron, in the adsorbent composition. In terms of processing aids, methylcellulose was used throughout to provide lubricity for the forming processes employed, as well as to increase the green strength of the uncalcined particles. A binder content of 10 wt% was used since previous work (Zheng et al. 2008) had shown this to be effective from the standpoint of achieving a high adsorbent weight fraction and acceptable particle strength.

After dry mixing, the materials were transferred to the agglomeration equipment and shaped into beads. A beaded form is preferred from the standpoint of bed packing efficiency. After forming was completed and beads of the target 16 × 20 mesh size were recovered by screening the particles, a calcination step was employed to set the binder and remove any combustible additives. Finally, to alter the basic composition of these zeolite adsorbents, an aqueous ion exchange process was used.

Two distinct bead forming methods were used, primarily to obtain products of different porosities. In the first method, an extrusion–spheronization process (see Barrett et al. 2006) was employed producing products of comparatively high porosity (~47–48 %). To produce products of lower porosity (~40–41 %) for comparison with the above, a Nauta forming method was used instead (Barrett and Stephenson 2011). For purposes of discussion, the

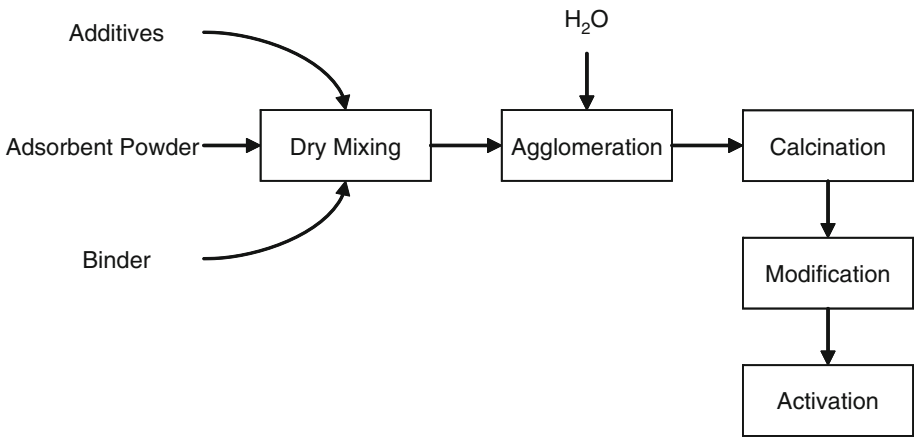

Fig. 3 Main steps used for laboratory sample preparation. In all cases, the "modification" step refers to ion exchange using chloride salts of Group I and II cations

higher porosity materials will be referred to as first generation materials and the lower porosity materials will be referred to as second generation materials.

For the extrusion–spheronization process, the following procedure was used: The raw materials included commercial zeolite A or LSX powders, Ludox LS colloidal silica binder, and a methylcellulose processing aid. These were all thoroughly mixed together in a Hobart planetary mixer for 60 min. Water was added to the above dry-mixed powder and mixing was continued until a paste had formed. The paste product was immediately extruded using a low pressure-dome extruder from LCI Corporation. The extrudates were converted to beads using a laboratory marumerizer (spheronizer) also from LCI Corporation. The products from several spheronizer batches were combined, screened to 16 × 20 mesh size and then calcined to set the binder, and remove the processing additive. The calcination was carried out using a shallow tray method by slowly increasing the temperature to 593 °C and holding at this temperature for 60 min under dry air having a dew point of −100 °C.

The lower porosity products were produced using a Nauta forming method. The raw materials above were combined and pre-mixed in the Hobart planetary mixer as before. This dry mixed raw material blend was transferred to a Nauta mixer with 1 in. diameter screw type auger and a conical shaped bowl having an internal volume of 1.5 ft^3. In the Nauta forming method, the combination of the auger rotation in two orthogonal directions, as well as the conical shaped mixing bowl, facilitate the formation of beaded products. Deionized water was added with constant stirring of the raw material blend in the Nauta mixer. At the end of the mixing time, beads including those in the target 16 × 20 mesh size range had formed. The products were screened and calcined using the shallow tray method under the same temperature ramp profile and set points described above.

The compositional variants of the Na, K-LSX beaded adsorbents prepared by both the extrusion–spheronization and Nauta forming processes (Barrett and Stephenson 2011) were prepared by ion exchange techniques. A column ion exchange method was employed to obtain ion exchange levels for the Group I and II cations of >98 % on a charge equivalents basis. The ion exchange column was made of glass and had a 3 in. inner diameter and a total volume of 1 L. The column includes a preheating zone with a thermocouple at the entrance to the column itself, to ensure that the solution has reached the intended ion exchange temperature, prior to coming in contact with the zeolite particles. Chemical analysis of all ion exchanged samples using inductively coupled plasma spectroscopy with proprietary analysis methodologies, except Ba-LSX for which a suitable standard was not available, was used to confirm that the samples had ion exchange levels >98 %. In all cases, the chloride salt of the incoming cation was used at 1.0 M concentration and fed to the ion exchange column at a flow rate of 15 mL/min. The cation exchange capacity of the LSX was assumed to be 5.75 meq/g and for Group I and II cations, a 3-fold excess of ion exchange solution was used for all cation exchanges, except for lithium. For Li as a consequence of its less favorable ion exchange isotherm, a 10-fold excess of ion exchange solution was employed instead. All ion exchanges were carried out at 90 °C on Na, K-LSX beads which had been rehydrated to a residual moisture content of at least 22 wt%. After the ion exchange was complete, the products were washed thoroughly with deionized water at a flow rate of 80 mL/min. A minimum of 50 L of deionized water was used for this washing step. A silver nitrate test was employed to indicate when the residual chloride had been washed out of the samples and the washing step could be terminated. Finally, the ion exchanged samples were activated under dry nitrogen using the shallow tray method at a temperature of 350 °C. Karl Fischer titration analysis was used to confirm that the residual moisture content of the samples from the activation process was <0.5 wt%.

2.2 Cryogenic breakthrough test system and method

A system capable of testing adsorbents for o-H_2 and p-H_2 separation at liquid nitrogen temperature (77 K) was custom designed and built. A schematic of the experimental system is shown in Fig. 4. The test system contains the following key components: liquid nitrogen Dewar, two independent series of adsorbent and catalyst beds, and a thermal conductivity analyzer specially calibrated to determine the o-H_2 and p-H_2 composition (Zhou et al. 2004). The material beds consist of stainless steel tubes, 21 in. × 1 in. OD, packed with either an o-H_2 to p-H_2 conversion catalyst or the adsorbent material under investigation, and are immersed in a liquid nitrogen bath to achieve the desired temperature. The beds are arranged as a set of two pairs, with each pair consisting of a catalyst bed placed upstream of an adsorbent bed. The purpose of the catalyst bed is to convert the hydrogen feed from n-H_2 to an equilibrium composition of approximately 50 % o-H_2 and 50 % p-H_2 at 77 K. If desired, the catalyst bed can be bypassed to examine the adsorbent performance for a n-H_2 feed. All lines were ¼ in. stainless steel and a 7-way valve was used to select the gas flow path from the following series of options: flow through catalyst bed 1 (or 2) and then adsorbent bed 1 (or 2), flow through adsorbent bed 1 or 2 directly with bypass of the catalyst bed and finally, bypass of both series of catalyst and adsorbent beds to enable feed flow directly to the analyzer for calibration. Type T thermocouples were placed throughout the system to measure the process gas temperature and the system pressure was controlled through the use of a pressure control valve. Each adsorbent and catalyst bed had a cooling loop to ensure that the process gas had sufficient time to equilibrate with the liquid nitrogen used throughout to provide cooling.

The efficacy of materials to produce an enriched p-H_2 product was evaluated using the breakthrough test method. The first step in the process is to ensure that the adsorbent material is in a suitable state for adsorption. For all initial experiments, this involved activating the adsorbent samples in dry nitrogen at 350 °C for zeolites and 250 °C for other non-zeolite types, loading the adsorbent samples into the

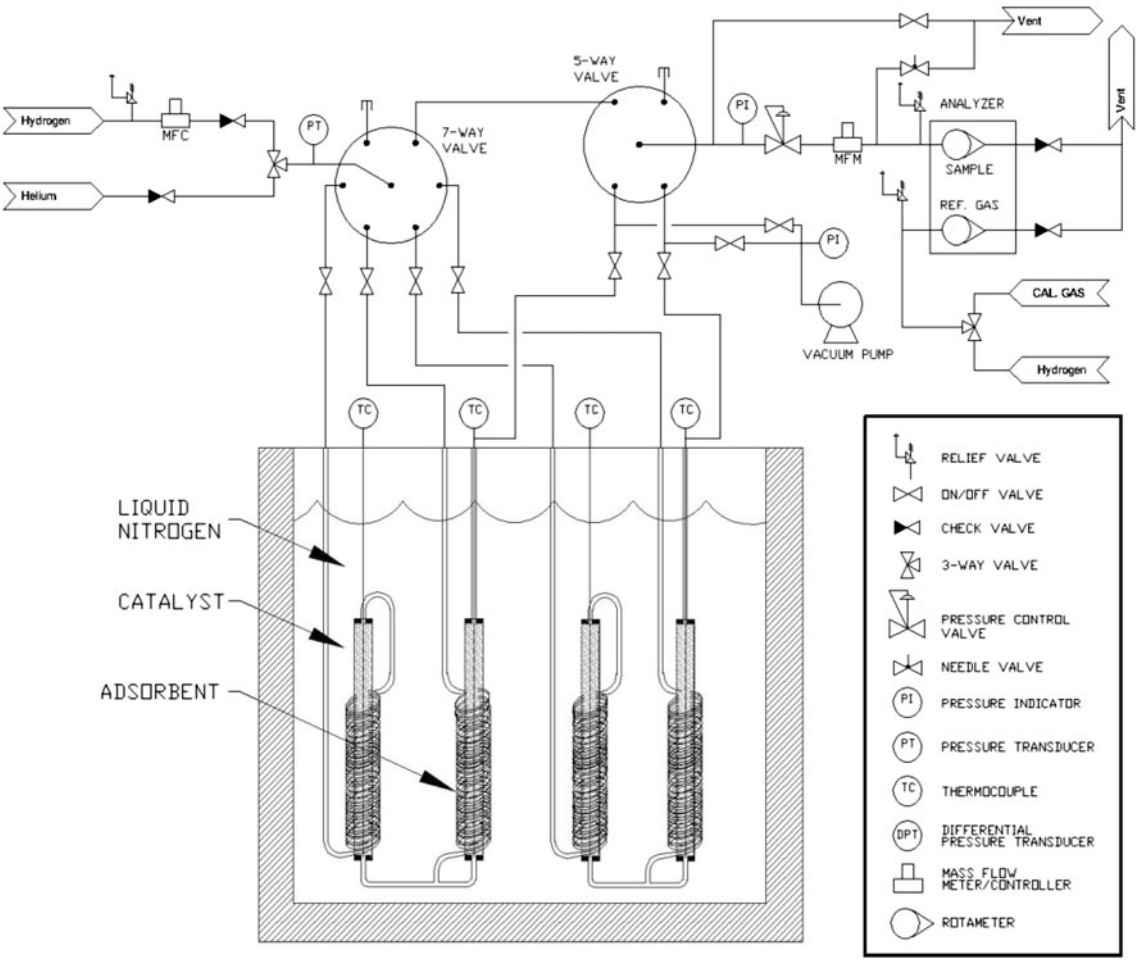

Fig. 4 Process and instrumentation diagram for the custom designed cryogenic breakthrough test system

adsorbent bed using a dry nitrogen purged glove box, to avoid any ambient moisture contamination, and, thereafter, connecting the adsorbent bed to the test system and evacuating the bed and system to at least 1×10^{-6} Torr. The purpose of the vacuum step was to remove any residual nitrogen from adsorbent and also from the test system. The Dewar was filled with liquid nitrogen at this stage, to achieve the desired separation temperature of 77 K. The n-H_2 (UHP grade) was then supplied to the process using a Porter mass flow controller and directed through a catalyst bed, consisting of hydrated iron oxide ($Fe(OH)_3$), upstream of the adsorbent bed to achieve an equilibrium mixture (at 77 K) of approximately 50 % o-H_2 and 50 % p-H_2 prior to contact with the adsorbent. For some tests, the catalyst bed was bypassed to examine the adsorbent performance for n-H_2 feed. The analyzer utilized in this system is a Teledyne 2000 series high sensitivity thermal conductivity analyzer. The breakthrough test pressure is controlled with a back pressure control valve located downstream of the catalyst and adsorbent beds.

In a typical breakthrough experiment, the n-H_2 gas flow was initiated firstly through the catalyst bed with the adsorbent bed thereafter exposed to the hydrogen gas exiting the catalyst bed. With reference to Fig. 5, the first part of the breakthrough test involves filling the system with hydrogen and raising the system pressure from vacuum to the test pressure which is controlled and set by the back pressure control valve, which remains closed until the set-point pressure is achieved. This constitutes the induction period. After the pressure set-point is achieved, the induction period is ended and flow through the test system begins. Any o-H_2 and p-H_2 concentration changes away from the catalyst baseline at this point are indicative of a separation of these two spin isomers, as a result of the presence of the adsorbent, which is able to create a new

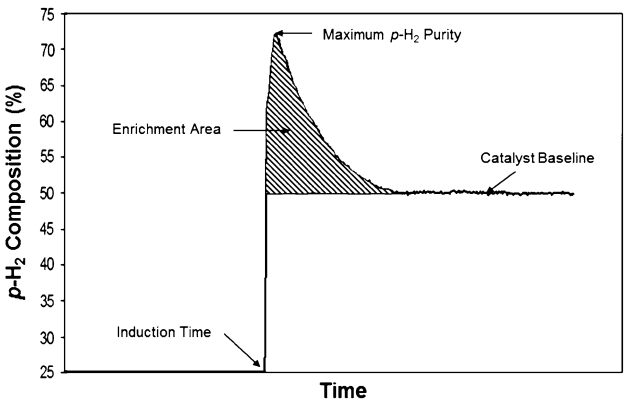

Fig. 5 Illustrative breakthrough curve with annotations to define the key characteristics used to assess adsorbent performance namely, maximum p-H_2 purity, enrichment area and catalytic baseline

o-H_2 and p-H_2 composition compared to that of the pure gas equilibrium. If the upstream catalyst bed is bypassed and the n-H_2 fed directly to the adsorbent bed, then the aforementioned o-H_2 and p-H_2 concentration changes will include both adsorptive and catalytic contributions, since the adsorbent compositions offer some degree of catalytic activity for o-H_2 to p-H_2 conversion. The purity in terms of spin isomer composition of the product hydrogen is highest initially and decreases with time as the adsorbent particles become saturated. When the o-H_2 and p-H_2 concentration returns to the catalyst baseline (or in the absence of the catalyst to the adsorbent catalytic baseline), the adsorbent capacity has been reached and no further separation takes place. The breakthrough experiment was ended after the o-H_2 and p-H_2 concentration remained at the catalyst baseline (or adsorbent catalytic baseline) value for an extended period of time. In terms of running a cyclic adsorption process, for example in a commercial system, the adsorbent bed would be regenerated prior to adsorbent saturation, with the feed being directed at this point to a previously regenerated bed which would start over from the induction period point shown in Fig. 5. In this way, a continuous purification process can be conceived.

From the % p-H_2 versus time curve obtained from the breakthrough test, two performance parameters namely maximum p-H_2 purity and enrichment area were obtained. The maximum p-H_2 purity, as the name suggests, is simply the peak purity of p-H_2 obtained during a given breakthrough experiment. The enrichment area is defined as the area corresponding to enrichment in p-H_2 above the catalyst baseline. These parameters are illustrated in Fig. 5 for a representative breakthrough curve obtained for a K-LSX sample, at the test temperature and pressure of 77 K and 40 psig, respectively. It is worthwhile noting that the breakthrough curves in Fig. 5 and elsewhere in this article are non-conventional in the sense that the breakthrough shown is for the preferred component, whereas in classical breakthrough experiments, the concentration of the undesirable specie or impurity is determined versus time. As plotted herein, the breakthrough curves depict the concentration versus time profiles for the preferred p-H_2. Since the mole fractions of o-H_2 and p-H_2 are equal to 1, a conventional breakthrough curve can be obtained from the data herein by plotting $1 - (\%\ p\text{-}H_2)$ versus time.

3 Results and discussion

3.1 o-H_2 to p-H_2 catalyst performance and intrinsic adsorbent catalytic activity

A first series of experiments was performed to follow up on the conclusions of Bystrov et al. (2006) who had shown

that many commercial adsorbents have high levels of catalytic activity for o-H_2 to p-H_2 conversion. The catalytic activity was attributed to the presence of paramagnetic impurities in the commercial zeolites in the form of transition metal and/or heavy metal species. A prerequisite for adsorbents to achieve this spin isomer separation is that they are substantially non-catalytic. It is hard to envisage that a high surface area adsorbent could be made to be entirely catalytically inert for this spin-inter-conversion catalysis, as a result of surface terminae and connectivity defects which exist in measurable concentrations in most classical adsorbents, including zeolites. This is particularly true in the light of the results from Minaev and Agren (1995) who proposed a new mechanism for o-H_2 to p-H_2 conversion, involving the formation of a collisional complex which induces spin uncoupling and leads to an effective Fermi contact hyperfine interaction between the *ortho* and *para* spin states upon contact with a paramagnetic species. This facile spin inter-conversion by collision of a hydrogen molecule with a paramagnetic surface (Matsunoto and Espenson 2005) will mean that many often catalytically inert materials will offer some conversion of spin isomers, such as o-H_2 and p-H_2. As a first step for the commissioning of our custom designed breakthrough test system, we ran a catalyst test of the commercial hydrated iron oxide obtained from Molecular Products, Inc. and verified that no p-H_2 enrichment takes place. The analyzer readings during this first test confirmed that the catalyst bed was sufficiently sized to equilibrate the feed to the 50 % p-H_2 and 50 % o-H_2 composition expected at 77 K, over the flow rate range 0.25–2.0 SLPM used in these experiments.

A commercial alumina adsorbent was tested next for its intrinsic catalytic activity. A sample of activated alumina at 7 × 14 mesh particle size was tested for its ability to catalyze the o-H_2 to p-H_2 conversion by bypassing the hydrated iron oxide catalyst bed and sending n-H_2 feed directly to the alumina adsorbent. The result showed that this adsorbent had some intrinsic catalytic activity for o-H_2 to p-H_2 conversion achieving a p-H_2 content of 38.0 % (see Table 1). A commercial Li-LSX adsorbent having a 1.5 mm average particle size was obtained from Zeochem LLC and tested next in the same way to determine its catalytic activity. The test results showed that commercial Li-LSX achieves a higher conversion, compared to alumina, with the p-H_2 content stabilizing at 44.3 %. The commercial Li-LSX adsorbent is beige colored and known to contain impurities, including iron compounds, which are believed to originate from the use of clay binding agents to form these commercial zeolites into agglomerates. To test whether or not at least part of the catalytic activity of the commercial Li-LSX adsorbent was derived from impurities present in the binding agent and/or from the clay binder itself, a sample of Li-LSX adsorbent was prepared from the same zeolite crystallites, but agglomerated instead using a colloidal silica binding agent (Ludox LS 30). The new sample was agglomerated using the extrusion–spheronization process and, as a result, had a porosity of 46–47 % which was higher than the commercial (clay-containing) Li-LSX sample from Zeochem having a porosity of 38 %. The catalytic activity test showed a reduction in catalytic activity of this colloidal silica bound Li-LSX with the p-H_2 content stabilizing at 33 % which is lower than even the commercial alumina sample. Since the crystallites of zeolite used in both the clay-bound commercial sample and the colloidal silica agglomerated lab-made sample were the same, it was concluded that the reduction in catalytic

Table 1 Catalysis testing results for candidate adsorbents for o-H_2 and p-H_2 separation at 77 K and 40 psig

Material	Binding agent type	Sample mass (g)[a]	Catalytic baseline (% p-H_2)[b]	Deviation from equilibrium (%)[c]
Commercial samples				
Catalyst[d]	N/A	100	50	0
Al_2O_3	N/A	151	38.0	24
Li-LSX	Clay	116	44.3	11.4
Laboratory prepared samples				
Li-LSX	Col. silica	128	33.3	33.4
Na-LSX	Col. silica	130	28.7	42.6
K-LSX	Col. silica	149	28.4	43.2
Cs-LSX	Col. silica	152	38.6	22.8
Ca-LSX	Col. silica	107	28.3	43.4
Na-A	Col. silica	148	31.0	38

[a] Mass of sample loaded into fixed volume sample tube

[b] For n-H_2 (25 % p-H_2) feed stream

[c] Devation from equilibrium composition of o-H_2 and p-H_2 at 77 K

[d] Where catalyst is hydrated iron oxide obtained from Molecular Products, Inc. which is used commercially for o-H_2 to p-H_2 conversion

activity was derived from the switch of the binding agent from clay to higher purity colloidal silica. As a result of this finding, all further adsorbent samples were prepared in agglomerated forms using only colloidal silica as the binding agent. A binder content of 10 wt% had proven to be effective in terms of producing particles with adequate crush strength and fast adsorption kinetics in previous work (Zheng et al. 2008) and the same binder content was adopted for the new samples prepared for o-H_2 and p-H_2 separation testing.

In order to determine whether or not different ion exchanged forms of the LSX influence the intrinsic catalytic activity for o-H_2 to p-H_2 conversion, different ion exchanged forms of the as-synthesized mixed cation Na, K-LSX zeolite were prepared by ion exchange of adsorbent beads formed using 10 wt% colloidal silica binding agent. From Group I, samples prepared included Li-LSX, Na-LSX, K-LSX and Cs-LSX where in each case, the ion exchange level was >98 %, and from Group II, Ca-LSX and was included in the sample set. The catalytic activity of all of these samples was tested, as described above, and the results are presented in Table 1.

The results obtained for this study of intrinsic catalytic activity for o-H_2 to p-H_2 conversion show that cation type also influences the degree of conversion achieved. For the Group I cations, the trend in catalytic activity appeared to correlate inversely with cation size with the order from most catalytic cation type to least being Li > Na > K. However, Cs-LSX had by far the greatest catalytic activity which deviates from the size correlation. The degree of catalytic activity for o-H_2 to p-H_2 conversion was low for the Ca-LSX sample showing that a divalent cation is not by default more catalytic than the corresponding Group I (monovalent) cation (i.e. Na-LSX and Ca-LSX achieve similar levels of o-H_2 to p-H_2 conversion). Finally, to briefly examine the impact of the zeolite framework architecture on the level of intrinsic catalytic activity for o-H_2 to p-H_2 spin isomer conversion, a sample of topologically related zeolite Na-A was prepared using the preferred colloidal silica binding agent at equivalent 10 wt% binder content for comparison with the Na-LSX. These two zeolites have silica/alumina ratios of 2 and their frameworks are built from the same sodalite cage secondary building unit. The structural differences between these two materials arises from the different stacking of the sodalite cages, giving the LSX a large pore size and a larger micropore volume, compared to the Na-A. Our results, concerning the amount of o-H_2 to p-H_2 conversion show that the Na-A has a slightly greater conversion than Na-LSX (31.0 % p-H_2 from Na-A vs 28.7 % from Na-LSX). From this comparison, it suggests that the zeolite framework density does play at least a small role in determining the catalytic activity of two structurally related and compositionally very similar zeolites.

To summarize the findings from our study of the catalytic activity of different adsorbent types for o-H_2 to p-H_2 conversion, binder type and especially any paramagnetic impurities contained therein, cation type and zeolite framework type all influence the intrinsic catalytic activity of the adsorbent. In terms of minimization of the residual catalytic activity, which is detrimental to the goal of o-H_2 and p-H_2 separation, zeolites are preferred to alumina, used previously as an adsorbent for this separation, zeolite X is preferred to smaller pore zeolite A and generally larger cations are beneficial especially Na, K and Ca types.

3.2 o-H_2 and p-H_2 breakthrough testing: back conversion study

Theoretically, o-H_2 and p-H_2 are intrinsically stable and possess infinite lifetimes (Anwar 2004). However, collisions with piping or vessel walls, trace impurities, and combinations thereof, serve to reduce the expected lifetime and promote conversion in the direction of equilibrium, at a given temperature. o-H_2 to p-H_2 conversion occurs readily over a catalyst at temperatures as low as 20 K (Schwartz et al. 2011). Many materials can effectively catalyze the reaction. Conversion at liquid hydrogen temperatures is known to produce sufficient heat to vaporize a significant portion of the liquid in a storage tank (Gursu et al. 1992). A series of tests were conducted to determine the extent of back-conversion of p-H_2 to o-H_2 at room temperature in our apparatus. The system was modified, as shown in Fig. 6, to collect product hydrogen from the hydrated iron oxide bed at 77 K (approximately 50 % p-H_2). A 2-L stainless steel holding tank was placed in parallel with the normal flow path just upstream of the analyzer. A valve on the top of the tank controlled whether the tank was in fill mode (collecting gas from the catalyst bed outlet) or purge mode (sending the collected gas to the analyzer). A vacuum pump was placed at the bottom opening to evacuate the tank prior to gas collection. At the start of the experiment, product gas from the catalyst bed was sent directly to the analyzer to ensure that the process was at steady-state and producing the expected 50 % p-H_2 product. Once this was established, flow was then directed into the collection tank, and the vessel was filled to a pressure of approximately 50 psig. The product gas was then left in the holding tank for a desired amount of time before sampling. After 65 h at room temperature and at the holding pressure of 50 psig, no change in the % p-H_2 was detected. This confirms that back-conversion of p-H_2 to o-H_2 in the exit lines of the reactor and the storage vessel was insignificant and that the analyzer results accurately measures the gas stream composition from either the catalyst or adsorbent bed. This test confirms that the p-H_2 to o-H_2 reaction is very slow without a catalyst, even at relatively high temperature.

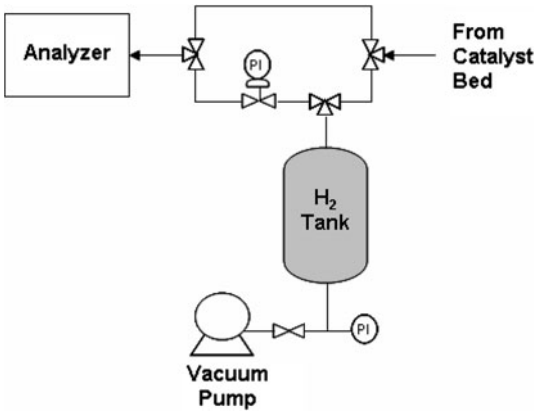

Fig. 6 Schematic of supplemental equipment added to the cryogenic breakthrough test system for the purpose of the enriched p-H_2 lifetime study

3.3 Adsorbent performance evaluation: first generation adsorbents with 46–47 % porosity

The first series of o-H_2 to p-H_2 separation testing was performed on the first generation adsorbents with comparatively high porosities, as prepared by the extrusion–spheronization method of agglomeration. One of the reasons for the high porosities of samples prepared using this method was identified as a consequence of the comparatively large amount of water required to prepare extrudable pastes from the preferred formulations comprising colloidal silica, as the binding agent. In all tests, the n-H_2 feed was directed through the hydrated iron oxide o-H_2 to p-H_2 conversion catalyst bed, which had been shown above to be sized sufficiently to achieve the expected conversion to 50 % p-H_2, expected at 77 K. Two additional samples were added to the test series used above for the catalytic activity study. Firstly, the as-synthesized Na, K-LSX was included since the catalysis study had suggested that Na and K cations offered amongst the lowest o-H_2 to p-H_2 hydrogen conversion activity. The Na, K-LSX form with Na:K $\sim$2:1 is obtained directly from the LSX synthesis and, as such, no extra ion exchange steps are required to obtain this adsorbent composition. Hence, this may be a lower cost option compared to either the Na-LSX or K-LSX, if the separation performance is adequate. Finally a Ba-LSX composition was also prepared to test whether or not larger Group II cations are preferred for this separation. The breakthrough test results (77 K and 40 psig) are presented in Table 2 using two metrics, namely the maximum p-H_2 purity measured and the enrichment area. The maximum p-H_2 purity is, as its name suggests, simply a measure of the peak purity achieved from a given adsorbent and test. The enrichment area equates to the productivity of the adsorbent to yield a p-H_2 product enriched beyond the 50 % p-H_2 equilibrium composition at 77 K.

From the data in Table 2 several observations can be made regarding the performance of the respective adsorbents to produce a p-H_2 enriched product. Firstly in accordance with the catalytic activity tests, the commercial adsorbents offer both inferior maximum p-H_2 purities, as well as lower enrichment areas. From the laboratory prepared LSX adsorbents having Group I charge balancing cations, the order of preferred cation type to least in terms of the maximum p-H_2 purity and enrichment area also follows the trend observed from the catalytic activity study: cation compositions with the lowest catalytic activity offer the best separation performance. From the separation testing, K-LSX offered the best overall performance achieving a maximum p-H_2 purity of 72.2 % and an enrichment area more than twice the commercial Li-LSX sample. From the Na-LSX, Na, K-LSX and K-LSX sample series where % K cation content are 0, 33 and >98 % respectively, it can be concluded that the separation performance is enhanced by the presence of greater levels of potassium charge balancing cations in the LSX structure. Another observation, potentially having some bearing on the separation mechanism, is the finding that the Cs-LSX sample performed better in the breakthrough separation test than expected based on the higher catalytic activity of this sample compared to other Group I cation containing LSX compositions.

Regarding the separation mechanism, a number of published works have consistently shown in both experiments and by theory that o-H_2 is preferentially adsorbed by conventional adsorbents, including zeolites, silicas and aluminas. The separation of o-H_2 and p-H_2 was first reported by Sandler (1954). Since, then a number of authors have attributed the separation to hindered rotation of the hydrogen molecule (e.g. Larin and Parbuzin 1992, White and Lassettre 1960). As stated by Anderson et al. (1999), hindered rotation is important since there is a correlation between the rotational state and the nuclear spin statistics that at sufficiently low temperatures is proposed to be modifiable by an adsorbing surface. Since p-H_2 has a nuclear state with a total spin of zero (antisymmetric spin state) it must exist in a symmetrical rotational state and vice versa for o-H_2. It is reasonable, therefore, that if an adsorbent surface leads to hindered rotational states, then an energetic preference would exist for the o-H_2 spin isomer leading, in turn, to some degree of separation depending on the adsorbent selectivity and capacity. A number of studies on adsorbed hydrogen in zeolites and related porous solids have shown that the microporous nature of these materials leads to modified rotational behavior for the adsorbed hydrogen. Modified 1-dimensional (hydrogen molecule rotating in alignment with internal micropore electrostatic fields) and 2-dimensional rotor (in plane rotation at surface sites) types have been

Table 2 Breakthrough testing results for candidate adsorbents for o-H_2 and p-H_2 separation at 77 K and 40 psig at 1 SLPM flow rate

Material	Binding agent type	Sample mass (g)[a]	Max p-H_2 purity (%)[b]	Enrichment area (% p-H_2 × sec)[b,c]
Commercial samples				
Catalyst[d]	N/A	100	50	0
Al_2O_3	N/A	151	53.4	699
Li-LSX	Clay	116	59.1	4,211
Laboratory prepared samples				
Li-LSX	Col. silica	128	68.8	6,974
Na-LSX	Col. silica	130	70.8	8,180
K-LSX	Col. silica	149	72.2	9,551
Na, K-LSX	Col. silica	141	72.1	8,842
Cs-LSX	Col. silica	152	72.1	8,053
Ca-LSX	Col. silica	107	64.1	4,813
Ba-LSX	Col. silica	151	66.9	6,530
Na-A	Col. silica	148	59.0	1,865

[a] Mass of sample loaded into fixed volume sample tube

[b] For feed stream at 50 % p-H_2

[c] Enrichment area is defined as the area corresponding to a p-H_2 content above the 50 % feed level in units of % p-H_2 × seconds obtained from the breakthrough test

[d] Where catalyst is hydrated iron oxide obtained from Molecular Products Inc. which is used commercially for o-H_2 to p-H_2 conversion

observed (Ramirez-Cuesta et al. 2000, 2007). Regarding the influence of different cation types, Kazansky et al. (1998) studied by diffuse reflectance IR spectroscopy, the adsorption of o-H_2 and p-H_2 on Li, Na-X (60 % Li), Na-X and Cs, Na-X (65 % Cs) zeolites at 77 K. The conclusions from Kazansky et al. (1998) from their IR study was that the degree of hindered rotation was most profound in the Li, Na-X sample and the least in the Cs, Na-X sample, where the rotation is nearly free. Our breakthrough testing results (see Table 2) showed improved separation for larger Group I cations, which from the observations of Kazansky et al. (1998) of near free rotation for the larger Cs cation, would appear to contravene the theoretical studies which call for hindered rotation to achieve the most separation. However, Kazansky et al. (1998) point out that the adsorption potential of a cation exchanged zeolite must include a component from the neighboring oxygen atoms of the framework, which is also influenced by the cation type. Hence, from the existing literature on the nature of the separation, it is likely that the cation type and local adsorption potential both influence the adsorption energy for o-H_2 and p-H_2 respectively. From our results on the alkali cation series, a larger cation seems to be preferred suggesting that a moderation of the extent of hindered rotation, coupled with an increase in the charge of the framework oxygen atoms, appear to enhance the separation performance. The higher oxygen charge of the Cs-LSX framework (Barthomeuf 1991) may explain why we see greater than expected separation performance from this sample, compared to that expected based on its higher catalytic activity. The K-LSX sample, which our testing showed to be preferred, may offer the best compromise in terms of degree of hindered rotation for the adsorbed hydrogen molecules, greater framework oxygen charge and lower catalytic activity.

Again with reference to Table 2, the Group II cation containing adsorbents Ca-LSX and Ba-LSX show a similar trend to the Group I samples. The performance of the Ba-LSX from the standpoint of maximum p-H_2 purity and enrichment area is superior to the Ca-LSX. Comparing the breakthrough test results for the Group I and II cation types, it is clear that all of the alkali metal cation containing LSX samples outperformed their alkaline earth counterparts. A plausible reason for the lower performance of the Group II cation containing LSX samples is the number of accessible cations is likely to be smaller for the divalent types. From the diffuse reflectance IR spectroscopy study of Kazansky et al. (1998), it was proposed that hydrogen at 77 K was able to adsorb at the SIII, SIII′ and SII cation positions in the LSX (for cation site designations, see Mortier 1982). According to these authors, no bands were observed attributable to hydrogen interactions with cations located deeper inside the sodalite cages at either the SI or SI′ positions. As a result, for the monovalent cations the level of cation exposure is essentially double that of the divalent cations (at the SiO_2/Al_2O_3 ratio of 2 in the monovalent case, the SII site is expected to be filled and accessible and additionally 2/3 of the available SIII positions are also likely to be occupied and exposed, whereas for the divalent cations, the exposed

cations are expected only at the filled SII position). Hence, a lower number of adsorption sites is expected for the Group II samples and our results clearly suggest this has important implications for the separation of o-H_2 and p-H_2.

Finally from the data in Table 2 we can comment on the performance of the Na-A adsorbent versus the Na-LSX. Our data show that the zeolite X structure is strongly preferred over the A-type. The reason for this is not obvious, especially since the level of catalytic activity of the Na-A was similar to the zeolite X samples prepared with the same binding agent and binder content. It is possible that the smaller size of the large cavity in the Na-A is less advantageous compared to the larger Faujasite supercage. Another reason could be differences in the cation location and degree of cation exposure between these two structures. To the best of our knowledge, there are no published crystal structures of Na-A at 77 K to compare with the published LSX structures, to ascertain whether the cation locations are different or the degree of cation exposure is lower in Na-A.

3.4 o-H_2 and p-H_2 breakthrough testing: impact of higher pressure

A new series of breakthrough tests was performed on each of the lab-made samples at 400 psig and 77 K instead of 40 psig and 77 K used for the performance testing described in the previous section. The motivation for the 400 psig testing was that this is closer to the operating conditions employed in a hydrogen liquefier. As an initial step, prior to running these higher pressure breakthrough tests, the performance of the commercial hydrated iron oxide bed was tested for its catalytic conversion using n-H_2 feed (25 % p-H_2) and found once again to be sized sufficiently to achieve the expected 50 % p-H_2 composition, at 77 K. Additionally, four of the adsorbent samples namely Na-LSX, K-LSX, Cs-LSX and Ca-LSX were also tested for their catalytic activity at 400 psig test pressure with n-H_2 feed. The results for both the catalyst testing and breakthrough testing are summarized in Table 3.

With reference to Tables 1 and 3 to compare the catalyst test results for the adsorbent samples with n-H_2 feed at 77 K at low and high pressure, respectively, we observe that for all four adsorbent samples, the catalytic conversion is slightly greater at the higher 400 psig pressure. For the four adsorbent samples, as a group, the catalytic conversion increased by approximately 1 % point at 400 psig versus the performance at 40 psig. The separation performance of all the adsorbents, however, is decreased significantly at 400 psig. The relative performance of the different adsorbents was similar to that observed at 40 psig. Once again, the largest enrichment area was achieved with K-LSX. The highest maximum p-H_2 purity, this time was achieved with Cs-LSX. At 77 K, the hydrogen isotherm for these LSX type adsorbents is not linear over the entire pressure range. Therefore, the ratio of available o-H_2 molecules in the gas phase to the number of available surface sites increases as the pressure is increased leading to less p-H_2 enrichment at higher pressures.

In addition to less p-H_2 enrichment, the high-pressure breakthroughs had much longer induction times. This is displayed in Fig. 7, which shows a comparison of the

Table 3 Breakthrough testing results for candidate adsorbents for o-H_2 and p-H_2 separation at 77 K and 400 psig at 1 SLPM flow rate

Material	Binding agent type	Sample mass (g)[a]	Catalytic baseline (% p-H_2)[b]	Max p-H_2 purity (%)[c]	Enrichment area (% p-H_2 × sec)[d]
Commercial catalyst sample					
Catalyst[e]	N/A	100	50	50	0
Laboratory prepared adsorbent samples					
Li-LSX	Col. silica	128	–	60.9	5,266
Na-LSX	Col. silica	130	29.3	61.3	6,098
K-LSX	Col. silica	149	29.4	63.5	8,133
Na, K-LSX	Col. silica	141	–	62.3	6,995
Cs-LSX	Col. silica	152	40.1	64.4	6,202
Ca-LSX	Col. silica	107	29.1	55.8	3,899
Ba-LSX	Col. silica	151	–	62.3	6,995

[a] Mass of sample loaded into fixed volume sample tube

[b] For feed stream at 25 % p-H_2

[c] For feed stream at 50 % p-H_2

[d] Enrichment area is defined as the area corresponding to a p-H_2 content above the 50 % feed level in units of % p-H_2 × seconds obtained from the breakthrough test

[e] Where Catalyst is hydrated iron oxide obtained from Molecular Products, Inc

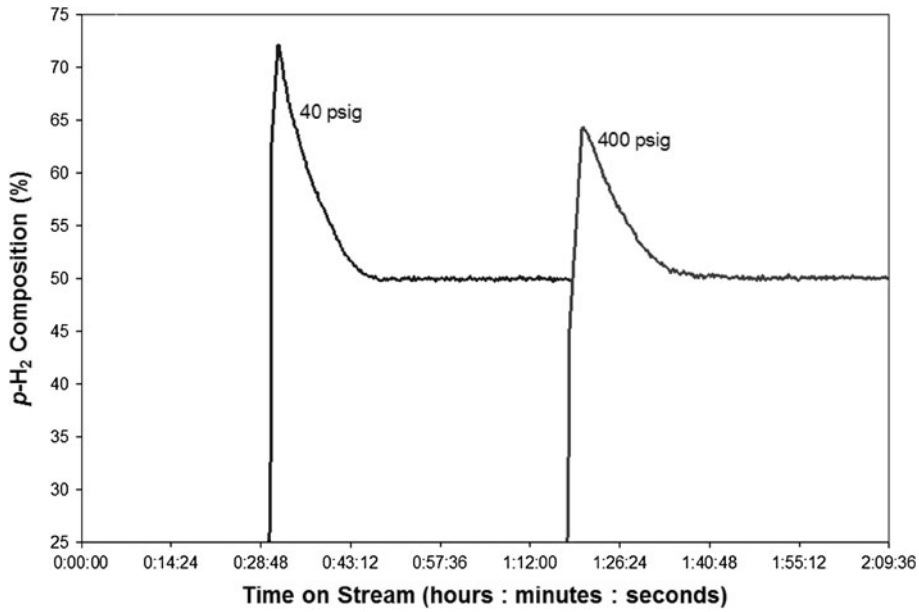

Fig. 7 Breakthrough curves for first generation adsorbent Cs-LSX at 77 K with feed flow of 1 SLPM at both 40 and 400 psig

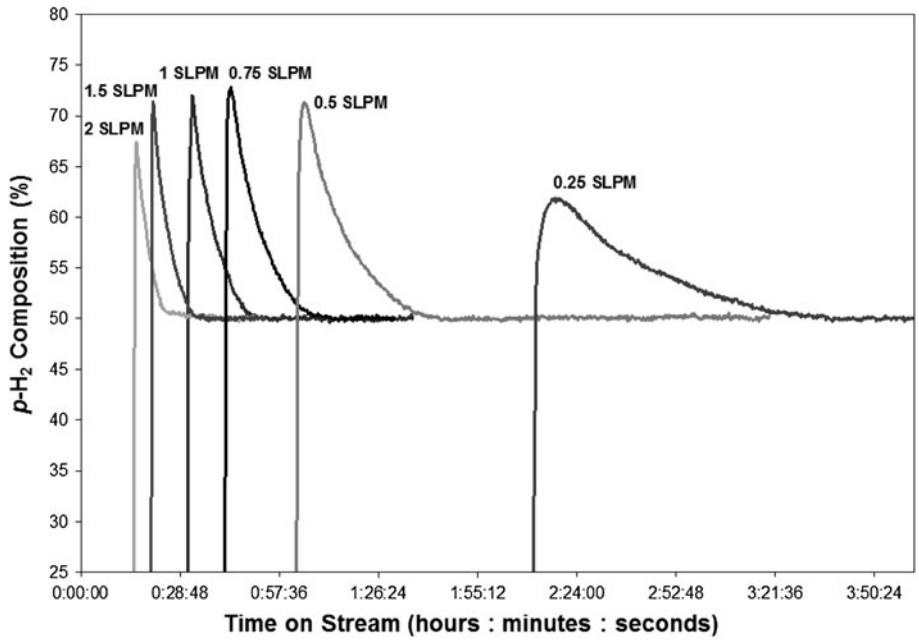

Fig. 8 Breakthrough curves for first generation adsorbent Na, K-LSX at 77 K and 40 psig as a function of different feed flow rates

breakthrough curves for Cs-LSX at both 40 and 400 psig at a hydrogen feed rate of 1 SLPM. The longer induction time is expected because the system pressure must increase to a much higher value before flow to the analyzer begins. The longer residence time is expected to lead to more mixing and axial diffusion in the system. This could explain why the peak at 400 psig is slightly wider than the peak at 40 psig. The mixing and diffusion could lower the measured maximum % p-H_2 purity because the highest purity produced has more time to mix with lower purity product before exiting the system to the analyzer.

3.5 o-H_2 and p-H_2 breakthrough testing: impact of feed flow rate

The effect of the hydrogen feed rate to the beds at 40 psig test pressure and 77 K temperature is displayed in Fig. 8 for the Na, K-LSX laboratory prepared zeolite adsorbent. The flow rate was both increased and decreased from the previous 1 SLPM value used throughout the basic separation performance testing described above. The maximum p-H_2 purity occurs in the range of 0.75 SLPM for the bed size tested. The dependence of the feed rate on enrichment

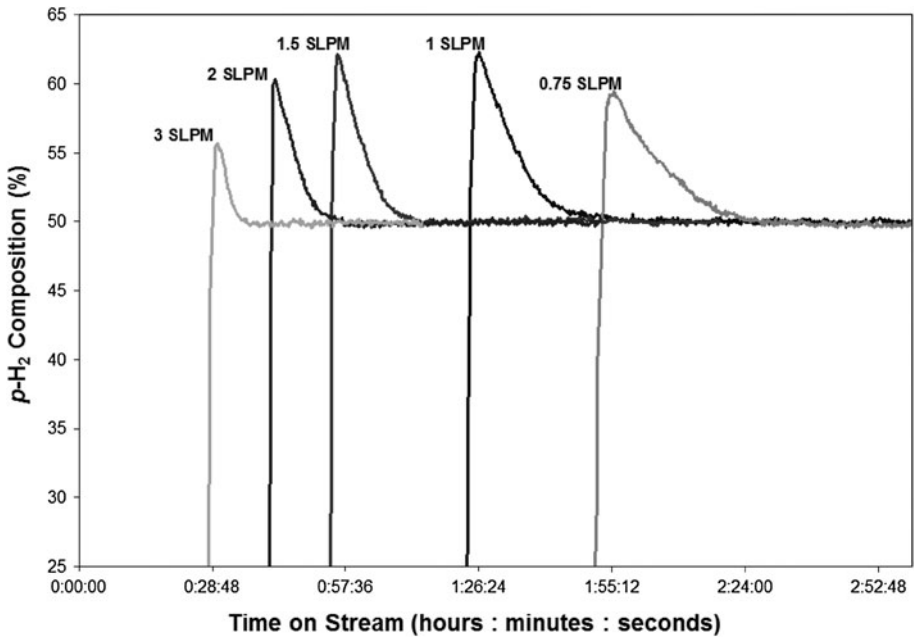

Fig. 9 Breakthrough curves for first generation adsorbent Na, K-LSX at 77 K and 400 psig as a function of different feed flow rates

is potentially due to both the rates of hydrogen adsorption and o-H_2 to p-H_2 conversion. If the feed rate is too high, insufficient adsorption occurs to achieve optimum enrichment. If the feed rate is too low, the additional residence time allows for more mixing and back-conversion of the enriched p-H_2 stream back towards the 50 % p-H_2 equilibrium composition. Another interesting aspect of this effect is that the shape of the breakthrough curve broadens as the feed rate is decreased, corresponding to an increase in residence time. This could be due to diffusion and/or mixing that occurs in the system. The potential presence of mixing effects makes it difficult to determine if the poor performance at low feed rates is due to unwanted catalysis, mixing, or a combination of the two.

The effect of feed rate on p-H_2 enrichment was also examined at 400 psig using the Na, K-LSX 16 × 20 mesh sample. The results of these experiments are shown in Fig. 9. As was observed at 40 psig, the enrichment and shape of the breakthrough curve were influenced by the feed rate with the maximum p-H_2 purity produced with a feed rate in the 1.0–1.5 SLPM range. This is a higher feed rate than shown in Fig. 8. At higher pressure, the same feed rate means a longer residence time in the system. At 400 psig, a 0.75 SLPM flow rate leads to too long a residence time, too much mixing and axial diffusion, and a peak that is too broad to show relatively high purity.

3.6 o-H_2 and p-H_2 hydrogen breakthrough testing: second generation adsorbent testing (impact of lower porosity)

The adsorbent screening study using the first generation materials with comparatively high porosities in the range 47–48 % had identified K-LSX as the most promising adsorbent for this separation. In order to try and increase the separation performance still further, a new K-LSX sample was made having a porosity in the range 40–41 %. Porosity reduction was considered important from the standpoint of maximizing the amount of active adsorbent per fixed volume adsorption bed. A different method of agglomeration was necessary to achieve the porosity reduction after repeated attempts to obtain denser colloidal silica bound adsorbents using the extrusion–spheronization process had been unsuccessful. Instead a Nauta forming method was used successfully with the preferred colloidal silica binding agent to prepare lower porosity LSX material at 1.0 mm average particle size. The calcination, potassium ion exchange and activation steps were carried out as described for the first generation adsorbents. The second generation K-LSX was tested using the breakthrough test method at low and high pressure and the results are compared to the first generation sample in Table 4.

From the data in Table 4 it is clear that the new low porosity K-LSX has significantly improved maximum p-H_2 purity and enrichment area. It is apparent that the enhancement in the maximum p-H_2 purity is more dramatic at lower pressure. This result is likely attributed to the nonlinearity of the adsorption isotherm, because the materials seem to exhibit similar catalytic behavior. However, the enrichment area is increased noticeably at both pressures, a result that can be attributed to the higher active site density of the second generation materials. The impact of different feed flow rates and pressures up to 400 psig was studied next for the second generation K-LSX adsorbent to see whether the performance can be

Table 4 Performance comparison of first and second generation K-LSX at 77 K

Material[a]	Low pressure[b,c]			High pressure (400 psig)[c]		
	Catalytic activity (% p-H_2)[d]	Max p-H_2 purity (% p-H_2)[e]	Enrichment area[e]	Catalytic activity (% p-H_2)[d]	Max p-H_2 purity (% p-H_2)[e]	Enrichment area[e]
1st Gen K-LSX	28.4	72.2	9,551	29.4	63.5	8,133
2nd Gen K-LSX	28.2	79.8	20,306	30.8	63.8	14,678

[a] Sample mass in same fixed volume test bed: 1st generation = 149 g and 2nd generation = 174 g

[b] Low pressure is 40 psig for 1st generation and 50 psig for 2nd generation

[c] Hydrogen feed rate was 1 SLPM for all tests shown in the table

[d] For n-H_2 feed (25 % p-H_2) stream-equilibrium is 50 % p-H_2

[e] For feed stream at 50 % p-H_2

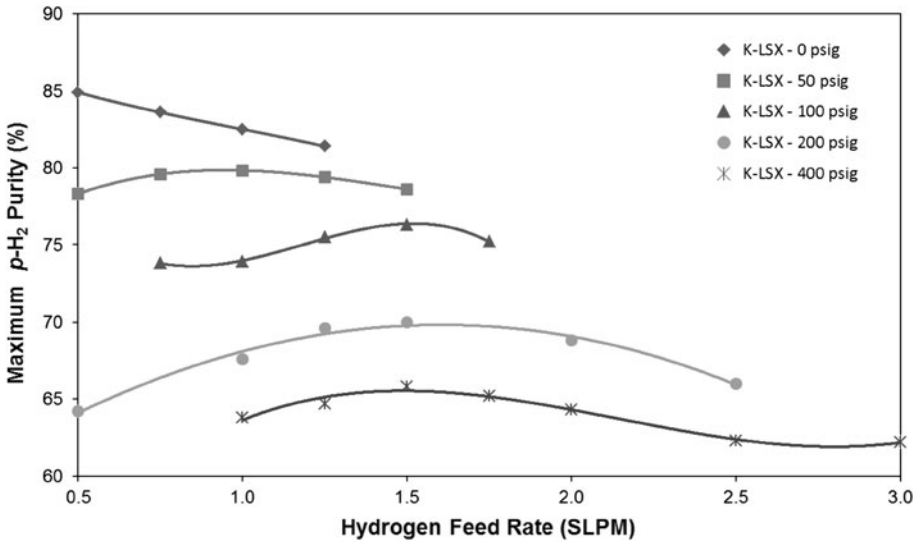

Fig. 10 Maximum p-H_2 purity for second generation adsorbent K-LSX at 77 K, at different feed pressures as a function of flow rate

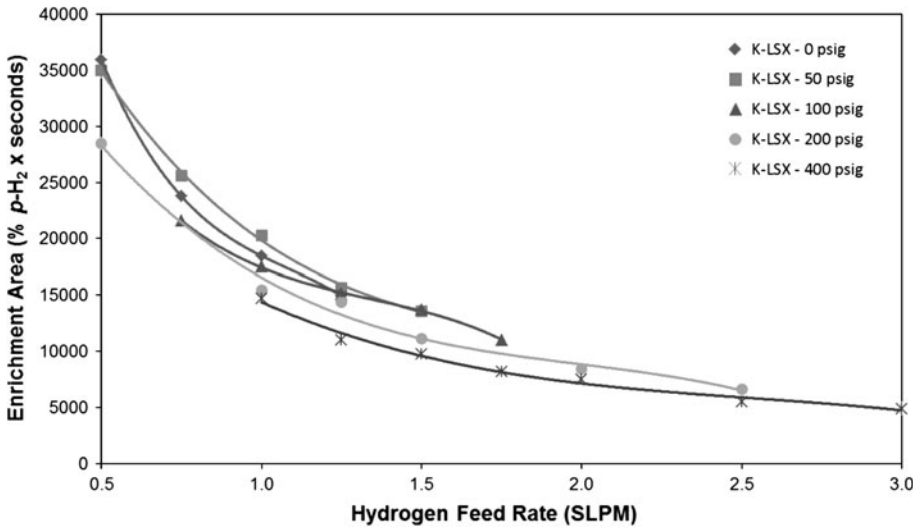

Fig. 11 Enrichment area for second generation adsorbent K-LSX at 77 K at different feed pressures as a function of feed flow rate

further optimized for this lower porosity material. The results obtained are summarized in Figs. 10 and 11. At ambient pressure and at the reduced flow rate of 0.5 SLPM, a maximum p-H_2 purity of 85 % and an enrichment factor of 36,000 in units of % p-H_2 × seconds were achieved. At 400 psig, close to the operating pressure of a hydrogen liquefier, the best maximum p-H_2 purity attained was 65 % at a flow rate of 1.5 SLPM which yielded an enrichment factor of 10,000 % p-H_2 × seconds.

4 Conclusions

An adsorbent screening study has been carried out to identify improved compositions for the separation of o-H_2 and p-H_2 at 77 K. Our agglomeration work showed that zeolites agglomerated using colloidal silica binding agents have lower catalytic activity for o-H_2 to p-H_2 conversion and this represents an important development versus traditional clay-bound commercial products, at nominally equivalent compositions. In terms of adsorbent selection, low silica zeolites of the LSX type were found to be preferred versus zeolites of type A and also activated alumina, which have both been used for this separation in the past. Modification of the colloidal silica bound LSX by ion exchange has been carried-out and the performance of the adsorbents has been tested, using a custom designed cryogenic breakthrough test system and method. The results show that potassium ion exchanged LSX offers the greatest performance in our two key metrics of maximum p-H_2 purity and enrichment factor (a term used to represent the adsorbent productivity). The preference for the K-LSX was rationalized in terms of the cation size, cation exposure, impact on hydrogen rotational motion and also on the resulting framework oxygen charge which are all suggested to play a role in maximizing the selectivity of the adsorbent towards o-H_2 and minimizing o-H_2 to p-H_2 catalytic conversion. From our breakthrough testing at 77 K, we found that the separation performance is best at low pressures and correspondingly low feed flow rates. Under these preferred conditions, maximum p-H_2 purities of 85 % have been achieved with excellent enrichment factors. However, at the operating pressures of most hydrogen liquefiers (400 psig), a potential home for this separation technology, the performance is significantly lower with the best maximum p-H_2 purity achieved being only 65 %, using the preferred colloidal silica bound K-LSX adsorbent with reduced macroporosity.

Acknowledgments This material is based upon work supported by the Department of Energy (National Nuclear Security Administration) under Award Number (DE-FG36-08GO18063/A000).

References

Anderson, C.-R., Coker, D.F., Eckert, J., Bug, A.L.R.: Computational study of molecular hydrogen in zeolite Na-A. 1. Potential energy surfaces and thermodynamic separation factors for *ortho* and *para* hydrogen. J. Chem. Phys. **111**, 7599–7613 (1999)

Anwar, M.S.: NMR quantum information processing with *para*-hydrogen, Ph.D. thesis, University of Oxford, UK (2004)

Baker, C.R., Shaner, R.L.: A study of the efficiency of hydrogen liquefaction. Int. J. Hydrogen Energy **3**, 321–334 (1978)

Barrett, P.A., Stephenson, N.A.: Adsorption properties of zeolites, zeolites and ordered porous solids: Fundamentals and applications. In: Martinez, C., Perez-Pariente, J. (eds.) Universidad Politecnica de Valencia, Valencia, pp. 67–90 (2011)

Barrett, P.A., Stephenson, N.A., Pontonio, S.J.: Gas separation adsorbents and manufacturing method. US Patent 2006082087 (2006)

Barthomeuf, D.: Acidity and basicity in zeolites. Stud. Surf. Sci. Catal. **65**, 157–169 (1991)

Brillyantov, N.A., Fradkov, A.B.: Degree of purification of hydrogen and helium by a chromatographic process on activated carbon. Zhurnal Sakharnoi Promyshlennosti **27**, 2404–2409 (1957)

Bystrov, V.P., Ivanov, E.B., Parbuzin, V.S.: *ortho–para* hydrogen and *para–ortho* deuterium separation factors on LiX zeolite at 50–112 K. Ars Separatoria Acta **4**, 37–42 (2006)

Clouter, M.J.: Application of a helium gas cryogenerator to the orthohydrogen separation process. J. Phys. E Sci. Instrum. **5**, 1099–1102 (1972)

Gursu, S., Lordgooei, M., Sherif, S.A., Veziroglu, T.N.: An optimization study of liquid hydrogen boil-off losses. Int. J. Hydrogen Energy **17**, 227–236 (1992)

Haubach, W.J., Knobler, C.M., Katorski, A., White, D.: The low temperature chromatographic separation of the isotopic hydrogens at 27 and 55 K. J. Phys. Chem. **71**, 1398–1402 (1967)

Haubach, W.J., Radakrishna, P., Katorski, A., Wang, R., White, D.: Isotope and *ortho–para* separations of the molecular hydrogens by adsorption at low temperatures, isotope effects in chemical processes. Adv. Chem. Ser. **89**, 73–98 (1969)

Kazansky, V.B., Jentoft, F.C., Karge, H.G.: First observation of vibration-rotation DRIFT spectra of *para*- and *ortho*-hydrogen adsorbed at 77 K on LiX, NaX and CsX zeolites. J. Chem. Soc. Faraday Trans. **94**, 1347–1351 (1998)

Larin, A.V., Parbuzin, V.S.: Theoretical estimate of ortho–para separation coefficients for H_2 and D_2 on A-type zeolites for small and medium coverage. Mol. Phys. **77**, 869–89, 1 (1992)

Matsunoto, M., Espenson, J.H.: Kinetics of the interconversion of parahydrogen and orthohydrogen catalyzed by paramagnetic complex ions. J. Am. Chem. Soc. **127**, 11447–11453 (2005)

Minaev, B.F., Agren, H.: Spin catalysis of *ortho–para* hydrogen conversion. J. Phys. Chem. **99**, 8936–8940 (1995)

Moore, W.R., Ward, H.R.: The separation of orthohydrogen and parahydrogen. J. Am. Chem. Soc. **80**, 2909–2910 (1958)

Mortier, W.J.: Compilation of Extra Framework Sites in Zeolites. Butterworth & Co., Gilford (1982)

Ramirez-Cuesta, A.J., Mitchell, P.C.H., Parker, S.F., Barrett, P.A.: Probing the internal structure of a cobalt aluminophosphate catalyst: An inelastic neutron scattering study of sorbed dihydrogen molecules behaving as one- and two-dimensional rotors. Chem. Commun. 1257–1258 (2000)

Ramirez-Cuesta, A.J., Mitchell, P.C.H., Ross, D.K., Georgiev, P.A., Anderson, P.A., Langmi, H.W., Book, D.: Dihydrogen in cation substituted zeolites X—An inelastic neutron scattering study. J. Mater. Chem. **17**, 2533–2539 (2007)

Sandler, Y.L.: The adsorption and *ortho–para* conversion of hydrogen on diamagnetic solids. II. The relative adsorbabilities of orthohydrogen and parahydrogen. J. Phys. Chem. **58**, 58–61 (1954)

Schwartz, J.M., Drnevich, R.F., Barrett, P.A., Neu, B.T.: Hydrogen liquefaction method and liquifier. US Patent 8,042,357 (2011)

Scott, R.B., Denton, W.H., Nicholls, C.M.: Technology and Uses of Hydrogen, p. 49. McMillian, New York (1964)

Singleton, A.H., Lapin, A.: Design of *para*–orthohydrogen catalytic reactors. Adv. Cryog. Eng. **11**, 611–630 (1965)

Silvera, I.: The solid molecular hydrogens in the condensed phase—fundamentals and static properties. Rev. Mod. Phys. **52**, 393–452 (1980)

Stevenson, R., Stevenson, D.: Simple chromatographic separation of para- and *ortho*-hydrogen and deuterium. J. Chromatogr. **234**, 231–233 (1982)

Van Cauwelaert, F.H., Hall, K.: Studies of the hydrogen held by solids XX. The chromatographic separation of the isotopic and allotropic hydrogens on alumina and fluorided alumina. J. Colloid Interface Sci. **38**, 138–151 (1972)

White, D., Haubach, W.J.: Separation of the hydrogen isotopes at 20.4 K. J. Chem. Phys. **30**, 1368–1369 (1959)

White, D., Lassettre, E.N.: Theory of *ortho–para* hydrogen separation by adsorption at low temperatures. J. Chem. Phys. **32**, 72–84 (1960)

White, D., Haubach, W.J., Lassettre, E.N.: *ortho–para* and isotope separations by preferential adsorption at low temperatures. J. Pure Appl. Chem. **2**, 323–324 (1961)

Zheng, J., Pontonio, S.J., Stephenson, N.A., Barrett, P.A.: High Rate High Crush Strength Adsorbents. US Patent 8,123,835 (2008)

Zhou, D., Ihas, G.G., Sullivan, N.S.: Determination of the *ortho–para* ratio in gaseous hydrogen mixtures. J. Low Temp. Phys. **114**, 401–406 (2004)